Hyper-Mobile Water Is Induced around Actin Filaments

Syed Rashel Kabir,* Keiichi Yokoyama,* Koshin Mihashi,† Takao Kodama,‡ and Makoto Suzuki*
*Department of Materials Science and Engineering, Graduate School of Engineering, Tohoku University, Sendai, Japan; †Faculty of Social and Information Sciences, Nihon Fukushi University, Aichi, Japan; and ‡Laboratory of Molecular Enzymology, Faculty of Information Science and Engineering, Kyushu Institute of Technology, Fukuoka, Japan

ABSTRACT When introduced into water, some molecules and ions (solutes) enforce the hydrogen-bonded network of neighboring water molecules that are thus restrained from thermal motions and are less mobile than those in the bulk phase (structure-making or positive hydration effect), and other solutes cause the opposite effect (structure-breaking or negative hydration effect). Using a method of microwave dielectric spectroscopy recently developed to measure the rotational mobility (dielectric relaxation frequency) of water hydrating proteins and the volume of hydration shells, the hydration of actin filament (F-actin) has been studied. The results indicate that F-actin exhibits both the structure-making and structure-breaking effects. Thus, apart from the water molecules with lowered rotational mobility that make up a typical hydration shell, there are other water molecules around the F-actin which have a much higher mobility than that of bulk water. No such dual hydration has been observed for myoglobin studied as the representative example of globular proteins which all showed qualitatively similar dielectric spectra. The volume fraction of the mobilized (hyper-mobile) water is roughly equal to that of the restrained water, which is two-thirds of the molecular volume of G-actin in size. The dielectric spectra of aqueous solutions of urea and potassium-halide salts have also been studied. The results suggest that urea and I^- induce the hyper-mobile states of water, which is consistent with their well-known structure-breaking effect. The molecular surface of actin is rich in negative charges, which along with its filamentous structure provides a structural basis for the induction of a hyper-mobile state of water. A possible implication of the findings of the present study is discussed in relation to the chemomechanical energy transduction through interaction with myosin in the presence of ATP.

INTRODUCTION

Protein-water interactions are key to biological functions (Mattos, 2002), among which those at the protein surface have the greatest relevance to stability, dynamics, and functions of proteins and hence have been extensively studied by a multitude of physico-chemical methods (Bellissent-Funel, 1999; Bryant, 1996; Gregory, 1995). Microwave dielectric spectroscopy is a powerful technique to investigate liquids, of which the structure and dynamics are dominated by intermolecular hydrogen bonds (for a review see Ellison et al., 1996). We have recently developed a method to measure the total volume of water molecules interacting with (hydrating) proteins in solution (dielectric exclusion volume or hydration-shell volume) as well as their rotational mobility (dielectric relaxation frequency, f_c) (Suzuki et al., 1996, 1997a; Yokoyama et al., 2001). For the globular proteins examined so far, the f_c values of hydrating water are in the range between 4 and 8 gigahertz (GHz) or lower, which is compared to the reported value of f_c for bulk water of 17 GHz at 20°C (Buchner et al., 1999). Those f_c values are equivalent to the dielectric relaxation times (τ_{diel}) $\geq$ 20–40 ps ($\tau_{diel} = 1/2\pi f_c$). In theory, $\tau_{diel} = 3\ \tau_c$ (Bloomfield, 2002; Fabelinskiĭ, 1997a), where τ_c is the orientational correlation time (residence time, the average time that a water molecule spends bound at a protein site) for water molecules hydrating protein surfaces estimated by nuclear-magnetic resonance-related methods (Bellissent-Funel, 1999; Halle and Denisov, 2001; Wüthrich, 2001). In addition, the number of hydrating water molecules per protein molecule (N_{total}) calculated from the dielectric exclusion volume agrees well with the solvent-accessible surface area-based estimate (N_{cal}) (Fig. 1). The data also gave an averaged value of the weight-based hydration (0.38 g/g protein), which falls within a range of values for various proteins estimated by other methods (Gregory, 1995; Zhou, 2001). Taken together, our dielectric method can provide the overall characteristics of the first hydration layer of proteins and the values are consistent with those obtained by other methods.

Using this dielectric method, the hydration of the myosin motor domain (S1) and its dynamic change during the ATP hydrolysis has been examined (Suzuki et al., 1997b). The result indicated that although S1 is not greatly different from other proteins in the total hydration level (see Fig. 1), the change of bound nucleotide ADP to ADP + P_i (ADP release followed by ATP binding and cleavage on addition of ATP) is accompanied by a small but substantial decrease (~5%) in the number of S-1 hydrating water molecules. It was then suggested that hydration and its dynamic change in motor proteins may play an important role in the underlying mechanism of muscle contraction. At the time, however, little information was available on the hydration properties of actin. Such information is essential to argue the mechanism of chemomechanical energy transduction in terms of water dynamics in S1-actin interaction (Highsmith et al., 1996).

In this study, we have extended the use of our dielectric method to actin solution. To achieve this, several difficulties had to be overcome in the recording of dielectric spectra, and

Submitted May 27, 2003, and accepted for publication August 8, 2003.

Address reprint requests to Makoto Suzuki, E-mail: msuzuki@argon.material.tohoku.ac.jp.

0006-3495/03/11/3154/08 $2.00

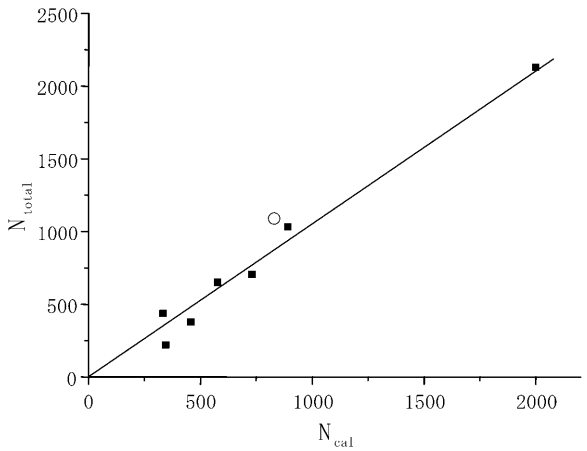

FIGURE 1 Hydration numbers of proteins estimated using dielectric spectroscopy. The ordinate (N_{total}) is the number of hydrating water molecules per protein molecule calculated from the dielectric exclusion volume, and the abscissa (N_{cal}) is the solvent-accessible surface areas (*ASA*)-based estimate. Data were from Yokoyama et al. (2001) and Suzuki et al. (1997b), for which the line was drawn by a linear regression analysis excluding the unfilled circle denoting a value for F-actin on the basis of its monomer unit estimated in this study (see Table 1).

the method of data analysis was elaborated. The results obtained indicate that the dielectric spectra of hydrated actin are distinct from those of proteins examined so far. In fact, it is virtually impossible to interpret the spectra without assuming that besides the lowered mobility of ordinary hydrating water, a component with much higher rotational mobility ($f_c \sim 40$ GHz) around the actin filaments (F-actin) exist. The dielectric exclusion volume is approximated to two-thirds of the molecular volume of globular monomer unit of F-actin (G-actin: M_r, 42.3 K). To check the validity of this finding, the dielectric spectra of solutions of urea and potassium-halides, KF, KCl, and KI were also measured. The hyper-mobile states of water are indeed induced in these solutions, which is consistent with well-known water-structure breaking effect of those solutes (Robinson et al., 1996).

Experimental and theoretical studies (Hribar et al., 2002; Tovchigrechko et al., 1999) suggest that the charge density of solute and the balance of strength between water-solute interaction and water-water hydrogen bond are major factors affecting structure of water around solute ions and molecules. Taking this into account, we have offered an explanation for how F-actin may enhance the mobility of the surrounding water molecules on the basis of its characteristic double-helix structure consisting of G-actin subunits with a negative charge-rich molecular surface. The rotational mobility of water molecules around solute molecules is directly related to their diffusibility and this is critical to translational motion of proteins (Bloomfield, 2002). Thus, a possible implication of the finding of the present study is also discussed in relation to chemomechanical energy transduction through interaction with myosin in the presence of ATP.

MATERIALS AND METHODS

Proteins and buffers

Actin was prepared from chicken pectoral and leg muscle (Spudich and Watt, 1971) and concentrated with Aquacide II (Calbiochem, San Diego, CA), which did not affect the polymerization capacity of actin. The protein concentration was determined from absorption at 290 nm with $A^{1\%}_{290nm} = 6.3\,cm^{-1}$ (Sheterline et al., 1998). Myoglobin was purchased from Sigma (St. Louis, MO). The low-salt buffer contained 2 mM HEPES (pH 7.2), 0.2 mM ATP, and 0.1 mM $CaCl_2$. This buffer was supplemented with KCl and $MgCl_2$ to make the high-salt buffer (2 mM HEPES, 0.2 mM ATP, 0.1 mM $CaCl_2$, 50 mM KCl, and 2 mM $MgCl_2$, at pH 7.2). The ratio of G- and F-actins was determined by fluorimetry using *n*-(1-pyrenyl)iodoacetamide (Kouyama and Mihashi, 1981). The partial specific volume (s_v) of proteins was calculated from the density of their solutions measured with an Anton-Paar (Graz, Austria) DMA-58 density meter.

Dielectric spectroscopy and data analysis

All measurements were made in a conically shaped glass cell (total volume, 3.2 ml) connected to a microwave network analyzer at 20.0 ± 0.01°C (Agilent, Palo Alto, CA, 8720C-85070A). The frequency-dependent signals were converted into complex dielectric spectrum consisting of real and imaginary parts, $\varepsilon^* = \varepsilon' - i\varepsilon''$ (Fig. 2). Noises inherent to the measuring system such as mismatching of cable-connectors as well as those from other sources and systematic interfering components were superimposed on the dielectric spectra. Thus, to overcome these noises the actual measurement and data processing were performed using the following three procedures. First, the spectra of the buffer ($\varepsilon_w^*(f)$) and protein solution ($\varepsilon_{ap}^*(f)$) were measured in pairs ~8–10× at a given protein concentration. The difference was taken for each pair (difference spectrum, protein solution vs. solvent buffer). The difference spectra obtained were then averaged and subjected to mathematical ''smoothing'' using fifth or higher order polynomial functions of $log_{10}f$. This gave the difference dielectric spectrum of the protein solution consisting of real and imaginary parts ($\Delta\varepsilon^*(f) = \Delta\varepsilon'(f) - i\Delta\varepsilon''(f)$) with greatly reduced noise level (Fig. 3 *a*). Secondly, there is a small inevitable difference in the free concentrations of ions between buffer and protein solution due to the binding of ions to proteins. This affects the imaginary part of the spectrum ($\Delta\varepsilon''(f)$) as an ionic conduction effect. This was corrected by subtracting $\Delta\sigma/(2\pi\varepsilon_0 f)$ ($\Delta\sigma$, the ionic conduction difference) from $\Delta\varepsilon''$ (Fig. 3 *a*). The value of D*s* was empirically determined to bring the absolute value of $\Delta\varepsilon''$ at 0.2GHz within the range between 0 and 1.0 in the present work. This correction gave little influence on the values of $\Delta\varepsilon'$ and $\Delta\varepsilon\approx$ in the frequency range between 2 and 20 GHz. Finally, the spectrum of the sample protein solution $\varepsilon_{ap}^*(f)$ was calculated by adding the difference spectrum ($\Delta\varepsilon^*(f)$) as estimated to the buffer spectrum ($\varepsilon_w^*(f)$), which had also been processed using the averaging and smoothing techniques described.

This ''back-synthesized'' spectrum $\varepsilon_{ap}^*(f)$ was analyzed as previously described (Yokoyama et al., 2001), with the exception that instead of using a spherical-solute model, a randomly oriented ellipsoidal-solute model was used as shown in Fig. 5 (Asami et al., 1980). The ellipsoid was assumed to have the major axis (*x*-axis) of $2r_x$ and the minor axis (*y*-axis) of $2r_y = 2r_z$ with a rotational symmetry around the major axis and double shells which cover the core ellipsoid coaxially. The major and minor axes of the shells are $2r_{xk}$ and $2r_{yk}$, where *k* is 1 or 2 corresponding to the first and second shell, respectively (Fig. 5). A constant axial ratio was adopted here as $q_0 = r_x / r_y = r_{x1} / r_{y1} = r_{x2} / r_{y2} \cdot q_0$ was assumed to be 30 for F-actin and 1.001 (quasi-unity, practically equivalent to a spherical model) for myoglobin. The complex dielectric constants ε_{q1}^*, ε_{q2}^* of the first and second shells were set by assuming a Debye-type relaxation function with relaxation frequencies f_{ck} and amplitudes δ_k as described in the following equations:

$$\varepsilon_{q1}^* = \varepsilon_{qinf1} + \delta_1/\{1 + i(f/f_{c1})\}, \quad (1)$$

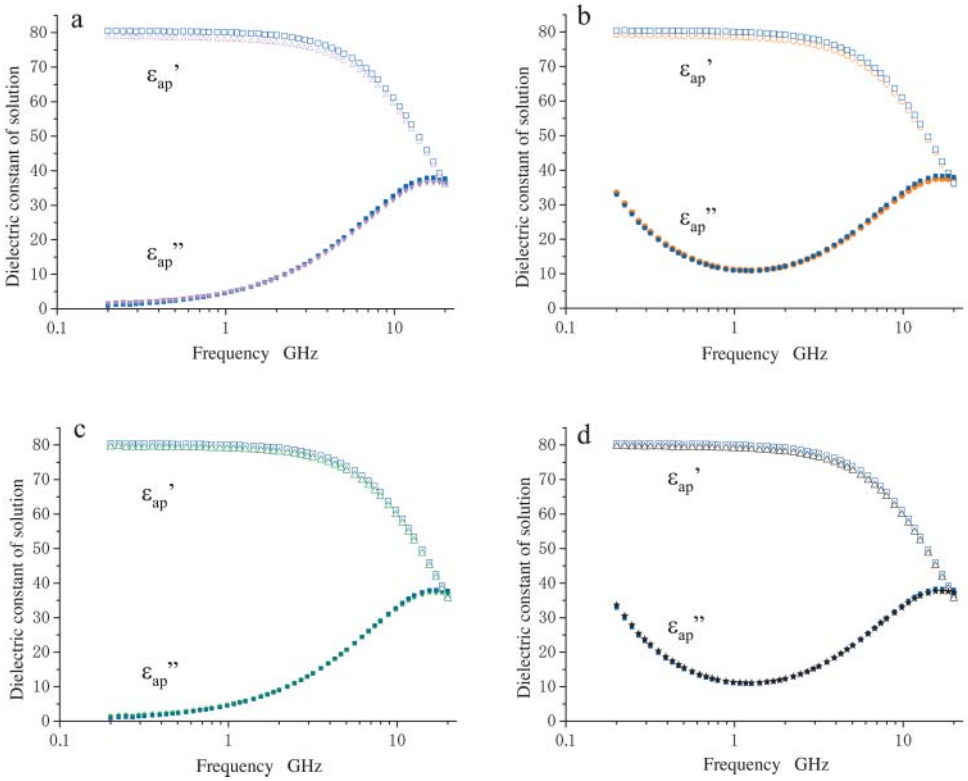

FIGURE 2 Dielectric spectra of actin and myoglobin solutions. Unfilled and solid symbols refer to the real and imaginary parts of dielectric spectra, respectively; blue symbols refer to buffers. (*a*) Spectra of actin (*magenta triangles*, 21.0 mg/ml) in the low-salt buffer (2 mM HEPES, 0.2 mM ATP, and 0.1 mM $CaCl_2$, at pH7.2). (*b*) Spectra of actin (*red circles*, 13.8 mg/ml) in the high-salt buffer (2 mM HEPES, 0.2 mM ATP, 0.1 mM $CaCl_2$, 50 mM KCl, and 2 mM $MgCl_2$, at pH 7.2). (*c*) Spectra of myoglobin (*green triangles*/*stars*, 14.0 mg/ml) in the low-salt buffer. (*d*) Spectra of myoglobin (*black triangles*/*stars*, 13.8 mg/ml) in the high-salt buffer.

$$\varepsilon_{q2}^{*} = \varepsilon_{qinf2} + \delta_2/\{1 + i(f/f_{c2})\}, \qquad (2)$$

where the dielectric constants of the shells at the high frequency limit ε_{qinf1}, ε_{qinf2} were set to 5.6 assuming that the values are close to that of free water (Kaatze, 1990). The dielectric constant of the model solution containing double-shelled ellipsoidal solutes ε_{aps}^{*} was then calculated using ε_{q1}^{*}, ε_{q2}^{*}, and ε_{w}^{*}, and the volume fraction of the double-shelled solute, ϕ_t, by the following equations derived from the method by Asami et al. (1980):

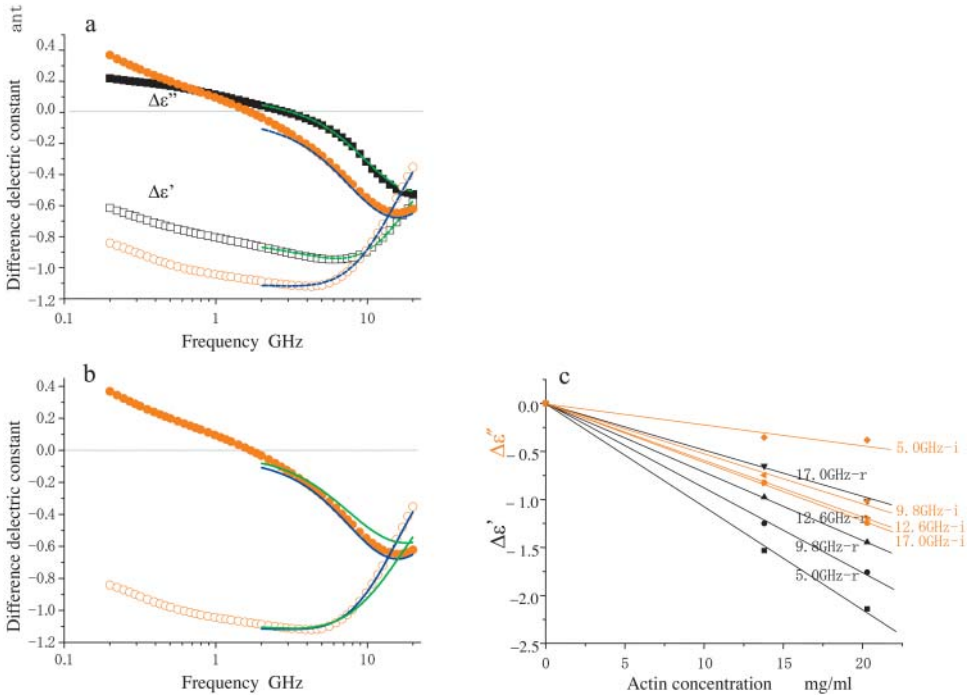

FIGURE 3 Difference dielectric spectra of F-actin (*red circles*) and myoglobin (*black squares*) solutions. Data were obtained from eight independent measurements for both proteins, averaged as described in Materials and Methods, and normalized to a protein concentration of 10 mg/ml. The size of the spectral symbols are roughly equal to the error widths. Unfilled and solid symbols refer to the real and imaginary parts of dielectric spectra as in Fig. 2. (*a*) Difference spectra ($\Delta\varepsilon'(f)$, $\Delta\varepsilon''(f)$) to show that actin and myoglobin are distinct. The theoretical curves for myoglobin were calculated according to Yokoyama et al. (2001) and those for F-actin by analysis using the model shown in Fig. 5. (*b*) Comparison of fit of theoretical curves: the single-shelled model, green solid lines; the double-shelled model, blue solid lines. (*c*) Protein concentration-dependence of $\Delta\varepsilon'$ (*black*) and $\Delta\varepsilon''$ (*red*) of F-actin at the frequencies indicated.

$$\begin{aligned}
\varepsilon^*_{aps} &= \varepsilon^*_w(2u^* + 1)/(1 - u^*)\\
u^* &= (\phi_t/9)(c^*_x + 2c^*_y)\\
c^*_x &= (\varepsilon^*_{qx} - \varepsilon^*_w)/\{\varepsilon^*_w + (\varepsilon^*_{qx} - \varepsilon^*_w)a_{0x}\}\\
c^*_y &= (\varepsilon^*_{qy} - \varepsilon^*_w)/\{\varepsilon^*_w + (\varepsilon^*_{qy} - \varepsilon^*_w)a_{0y}\}\\
a_{0x} &= -(q_0^2 - 1)^{-1} + q_0(q_0^2 - 1)^{-3/2}\\
&\quad \times \log\{q_0 + (q_0^2 - 1)^{1/2}\}\\
a_{0y} &= a_{0z} = (1 - a_{0x})/2,
\end{aligned} \tag{3}$$

where ε^*_{qx}, and ε^*_{qy} are given by

$$\begin{aligned}
\varepsilon^*_{qx} &= \varepsilon^*_{q2}\frac{\varepsilon^*_{q2} + (\varepsilon^*_{q1x} - \varepsilon^*_{q2})a_{0x} + \lambda(\varepsilon^*_{q1x} - \varepsilon^*_{q2})(1 - a_{0x})}{\varepsilon^*_{q2} + (\varepsilon^*_{q1x} - \varepsilon^*_{q2})a_{0x} - \lambda(\varepsilon^*_{q1x} - \varepsilon^*_{q2})a_{0x}}\\
\varepsilon^*_{qy} &= \varepsilon^*_{q2}\frac{\varepsilon^*_{q2} + (\varepsilon^*_{q1y} - \varepsilon^*_{q2})a_{0y} + \lambda(\varepsilon^*_{q1y} - \varepsilon^*_{q2})(1 - a_{0y})}{\varepsilon^*_{q2} + (\varepsilon^*_{q1y} - \varepsilon^*_{q2})a_{0y} - \lambda(\varepsilon^*_{q1y} - \varepsilon^*_{q2})a_{0y}}\\
\varepsilon^*_{q1x} &= \varepsilon^*_{q1}\frac{\varepsilon^*_{q1} + (\varepsilon_p - \varepsilon^*_{q1})a_{0x} + \mu(\varepsilon_p - \varepsilon^*_{q1})(1 - a_{0x})}{\varepsilon^*_{q1} + (\varepsilon_p - \varepsilon^*_{q1})a_{0x} - \mu(\varepsilon_p - \varepsilon^*_{q1})a_{0x}}\\
\varepsilon^*_{q1y} &= \varepsilon^*_{q1}\frac{\varepsilon^*_{q1} + (\varepsilon_p - \varepsilon^*_{q1})a_{0y} + \mu(\varepsilon_p - \varepsilon^*_{q1})(1 - a_{0y})}{\varepsilon^*_{q1} + (\varepsilon_p - \varepsilon^*_{q1})a_{0y} - \mu(\varepsilon_p - \varepsilon^*_{q1})a_{0y}}.
\end{aligned} \tag{4}$$

where $\lambda = (v + \phi_1)/\phi_t = r_{x1}r^2_{y1}/r_{x2}r^2_{y2}$, $\mu = v/(v + \phi_1) = r_x r^2_y/r_{x1}r^2_{y1}$, ϕ_1 is the volume fraction of the first shell in the solution, and v is the volume fraction of the core ellipsoid. The values of f_{c1}, δ_1, and ϕ_1 were determined as adjustable parameters by least-square fitting to the real part $\Delta\varepsilon'$ in the frequency range between 2 and 10 GHz. Using this parameter set of the first Debye component, the second set of adjustable parameters, f_{c2}, δ_2, and ϕ_2 was determined by least-square fitting taking into account the ϕ_2-effect on $\Delta\varepsilon'$ for ~10–14 GHz, and the f_{c2}-effect on $\Delta\varepsilon''$ for ~12–20 GHz. The entire set of parameters (f_{c1}, δ_1, ϕ_1;f_{c2}, δ_2, ϕ_2) thus obtained was used as the initial estimates for the second stage of fitting, which was repeated until no further improvement resulted. Thus, the total volume fraction of the hydrated solute ϕ_t ($= v + \phi_1 + \phi_2$) could be determined. Finally, assuming that F-actin solution is a one-solute/one-solvent system, the apparent dielectric constant of the double-shelled ellipsoid, ε^*_q, was calculated from the experimental values of ε^*_{ap}, ε^*_w, and the value of ϕ_t by the following equations:

$$\begin{aligned}
\varepsilon^*_q &= \varepsilon^*_w + \{-b^* - (b^{*2} - 4a^*c^*)^{+1/2}\}/2a^*\\
a^* &= a_{0x}a_{0y}s^* - 2a_{0x} - a_{0y}\\
b^* &= \{s^*(a_{0x} + a_{0y}) - 3\}\varepsilon^*_w\\
c^* &= s^*(\varepsilon^*_w)^2\\
s^* &= (9/\phi_t)(\varepsilon^*_{ap} - \varepsilon^*_w)/(\varepsilon^*_{ap} + 2\varepsilon^*_w).
\end{aligned} \tag{5}$$

RESULTS AND DISCUSSION

Dielectric spectra of actin solutions

Dielectric spectra of the actin solution (the real part, ε'_{ap} + the imaginary part, ε''_{ap}) in the low-salt buffer recorded after being introduced into the measuring cell (Fig. 2 *a*) were very similar to those of other globular proteins (Yokoyama et al., 2001), among which myoglobin was chosen as a reference protein in the present study (Fig. 2 *c*). When the concentration of actin exceeds ~4 mg/ml, the extra actins assemble into filaments even at low ionic strengths (Sheterline et al., 1998). Using a fluorimetry technique, it was determined that a mol fraction of F-actin exceeded 45% in the low-salt buffer at actin concentrations >10 mg/ml, which was a prerequisite for successful dielectric measurements. Hence, after introducing the actin into the measuring cell, the actin was completely polymerized by adding KCl + $MgCl_2$. Measurements were then made using the high-salt buffer as the reference (Fig. 2 *b*). In the low frequency region (<2 GHz) the ionic conduction effect could be observed on the imaginary part (ε''_{ap}). The spectra were not substantially different from those recorded in the low-salt buffer. These observations also apply to the myoglobin spectra (Fig. 2 *d*).

A small but systematic difference between the dielectric spectra of the protein solution and the buffer seen over the frequency range investigated (Fig. 2) is a reflection of the difference in polarizability between the hydrated protein and the solvent. This is clearly shown in the difference spectra (Fig. 3 *a*: $\Delta\varepsilon^*(f)$). The description from here onward is based on the analysis of the dielectric spectra, which was limited in the frequency range above 2 GHz for two reasons. First, the effect of ionic conduction difference between protein and buffer solutions could not be completely removed from the spectra in the lower frequency range. Second, some relaxation phenomena such as subdomain fluctuation of a large protein (Hayashi et al., 2000) or orientation relaxation of molecular dipoles of amino acids (Suzuki et al., 1997a) were observed in the range <1 GHz. The effects of these relaxation irrelevant to the rotational mobility of water can be minimized, if not totally excluded, by the analysis in the frequency range >2 GHz.

As for the real-part spectrum, $\Delta\varepsilon'(f)$, in the frequency range >2 GHz, actin stays below that of myoglobin up to 9 GHz, but then rises more steeply thereafter. Corresponding to this, the pattern of the actin imaginary part, $\Delta\varepsilon''(f)$, is clearly distinct from that of myoglobin. It should be noted that both the $\Delta\varepsilon'$ and $\Delta\varepsilon''$ values calculated at the different frequencies are proportional to the actin concentration (Fig. 3 *c*). The magnitudes of standard errors of both $\Delta\varepsilon'$ and $\Delta\varepsilon''$ were in a range between 0.010 and 0.027.

Dielectric characterization of hydrated actin

In the spectrum of the hydrated solutes at frequencies >2 GHz (Fig. 4 *a*), the real-part $\varepsilon'_q(f)$ of the actin spectrum (*circles*) decreased gradually. Accompanying this change was a slow increase of the imaginary-part $\varepsilon''_q(f)$, whereas myoglobin (*squares*) $\varepsilon''_q(f)$ showed a broad but clear peak at 7 GHz. The actin spectra in the low (*triangles*) and high-salt (*circles*) buffers are similar (Fig. 4 *b*) but different from the myoglobin spectra (Fig. 4 *c*). Among the proteins other than actin examined so far (Yokoyama et al., 2001), bovine serum albumin and ovalbumin showed the myoglobin-type spectra irrespective of the buffer used, i.e., low- or high-salt (data not shown). Thus, the dielectric characteristics of actin solution are genuine, and cannot be ascribed to an effect of ionic strength.

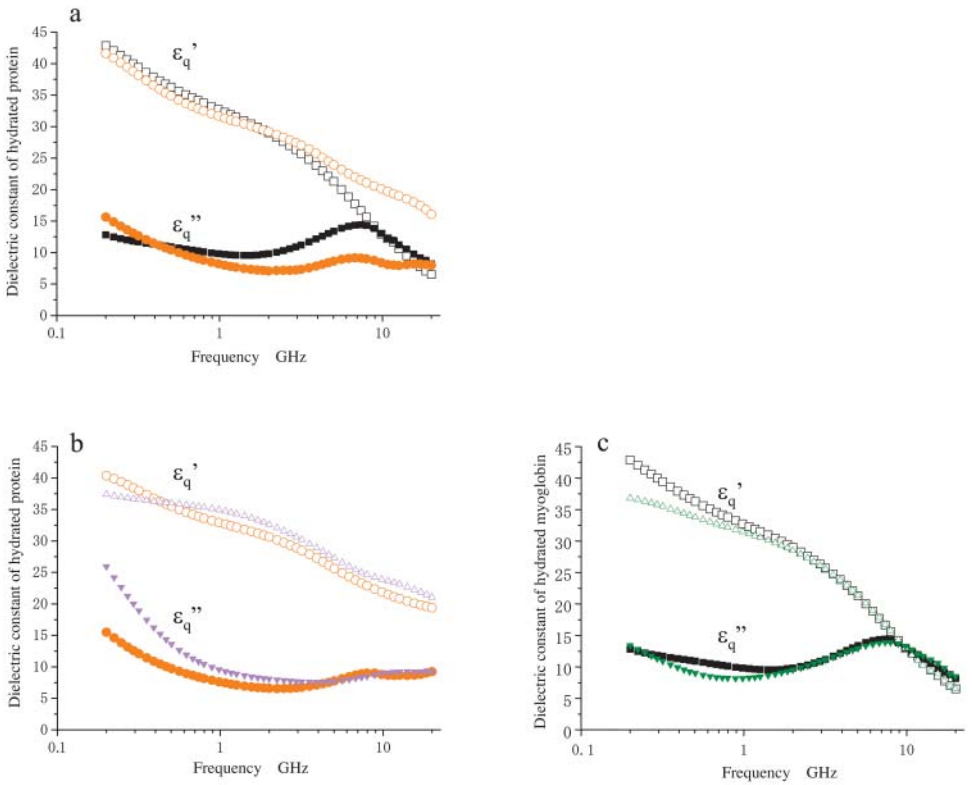

FIGURE 4 Dielectric spectra ($\varepsilon_q^*(f)$) of hydrated F-actin and myoglobin. Unfilled and solid symbols refer to the real and imaginary parts of dielectric spectra as in Fig. 2. (*a*) Comparison of actin (*red circles*) and myoglobin (*black squares*) in the high-salt buffer. (*b*) Comparison of actin in the low-salt buffer (*magenta triangles*) and the high-salt buffer (*red circles*). (*c*) Comparison of myoglobin in the low-salt buffer (*green triangles*) and the high-salt buffer (*black squares*).

Double-shelled model for analysis of actin spectra

A single-shelled sphere model describes well the dielectric spectra for non-actin globular proteins (Yokoyama et al., 2001), as illustrated by the theoretical curve (*green solid lines*) obtained for myoglobin (Fig. 3 *a*). In contrast, it was not possible to obtain any satisfactory theoretical spectra of actin no matter what dielectric parameters were chosen, which was clearly shown by systematic deviations of the best fitted theoretical curves (*green solid lines* in Fig. 3 *b*) from the observed spectra between 2 GHz and 10 GHz. Hence, a more complex analysis was attempted using the concept of a double-shelled ellipsoidal solute consisting of an actin filament surrounded by two layers of hydrating water, each of which had characteristic dielectric properties (Fig. 5). This analysis provided satisfactory fitting curves (*blue solid lines*) for the observed difference spectrum of actin (Fig. 3, *a* and *b*).

Thus, a unique feature of actin hydration has emerged (Table 1). The number of water molecules for every G-actin

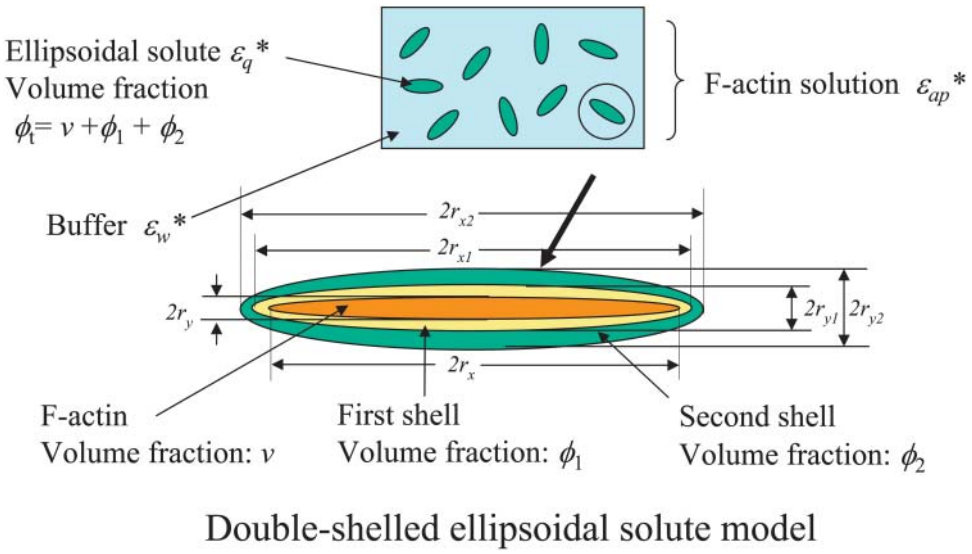

FIGURE 5 Double-shelled ellipsoidal solute model. This model (Asami et al., 1980) was used to analyze the dielectric spectrum of F-actin solution as outlined in Materials and Methods. The expressions $2r_x$ and $2r_y$ refer to the lengths of major and minor axes of the ellipsoidal shells, respectively. Theoretical spectral curves obtained were superimposed on the observed values for $\Delta\varepsilon'(f)$ and $\Delta\varepsilon''(f)$ (*blue-colored solid lines* in Fig. 3 *a*). Note that when applied to the spectrum of the myoglobin solution with the protein axial ratio of 1.001, a curve essentially the same as estimated by the previous method was obtained (Yokoyama et al., 2001).

TABLE 1 Dielectric parameters for hydration of F-actin and myoglobin

Relaxation component	1st				2nd		
Protein	f_{c1} (GHz)	δ_1	ϕ_1/c*	N_1	f_{c2} (GHz)	δ_2	ϕ_2/c*
F-actin†	6.5	45	0.506	1190	40	75	0.600
Myoglobin	6.2	79	0.588	581‡	–	–	–

*$N_1 = \phi_1 M_w/18c$, where M_w is mass weight of protein. See text for other details. c is the protein concentration (g/ml). The values of the partial specific volume s_v (F-actin, 0.743 ml/g; myoglobin, 0.74 ml/g) were measured with a density meter (Anton Paar DMA-58). ϕ_1/c and ϕ_2/c are the volume fractions of the hydration shells per unit protein concentration.

†The values were calculated from the averaged and smoothed spectrum as described in Materials and Methods. The individual spectra (not averaged but smoothed) were also analyzed to estimate the errors accompanying the best-fit values given here to show the precision of eight independent measurements. The means were almost identical to the values obtained for the averaged spectrum, and the relative standard errors of the means for f_{c1}, δ_1, and ϕ_1 were 3.0%, 4.0%, and 3.0%, respectively, and those for f_{c2}, δ_2, and ϕ_2 were 4.6%, 4.8%, and 7.0%, respectively.

‡This value was much larger than the one reported previously (~380). This discrepancy is most likely due to the difference in the frequency range employed, 2–20 GHz in the present work compared to the earlier of 2–10 GHz. Increasing the frequency range may be equivalent to taking into account the hydrating water with a higher mobility. Taking into consideration weakly and strongly restrained water (Suzuki et al., 1996; Yokoyama et al., 2001), these values are roughly consistent with those estimated by MD calculations (Makarov et al., 2000).

unit in the first hydration shell (N_1) is slightly excess to make the mono-layer covering the three-dimensional structure model of G-actin unit in F-actin (Lorenz et al., 1993). The volume fraction of the second shell with a high f_c is approximately two-thirds of the molecular volume of G-actin. Judging from its dielectric parameters, it seems almost impossible to postulate that any substance other than water could constitute this second shell. In this context, it seems appropriate to give a rough sketch of the hydration profile of F-actin. Assuming a filament as a straight cylinder with smooth surface, its radius would be 2.6 nm or 3.3 nm inclusive of the first hydration shell (see above). If the hyper-mobile water molecules were evenly distributed on the surface of cylinder, the overall radius could be 3.9 nm. However, such even distribution, which is most likely for the restrained water constituting the first hydration shell as judged from the linear relationship between N_{total} and N_{cal} (Fig. 1), is by no means realistic for the hyper-mobile water, because the molecular shape and chemical nature of the protein surface are very complex. In addition, it is not known yet where water molecules are hyper-mobilized on the actin surface (see below) or how they exchange with those of lower mobilities.

Hyper-mobile water around solute molecules

A state where water has a mobility higher than that of the bulk water (here we refer to as hyper-mobile water) was first hypothesized to explain hydration anomalies of some ions such as I^- and Cs^+. This effect has been referred to as water-structure breaking (Frank and Wen, 1957) or negative hydration (Samoilov, 1957). For diluted solution of urea (Tovchigrechko et al., 1999) and solutions of alkali-halide salts (Collins, 1997; Hribar et al., 2002; Imai et al. 2002), experimental and theoretical (computational) studies indicated that this effect was attributable to the charge density of the solute and the balance of strength between water-solute interaction and water-water hydrogen bond. We measured the dielectric spectrum of a urea solution (Fig. 6 *a*), which could only be explained assuming a dipole with an f_c value of 30 GHz in addition to the low frequency component (f_c = 6.5 GHz, probably the urea dipole itself and weakly restrained water together). Dielectric measurements and analysis were also made for solutions of potassium halide-salts, KF, KCl, and KI. The results were similar to those obtained for urea. Thus, I^- and Cl^- but not F^- seemed to induce some high frequency component(s) and I^- showed a much stronger effect (Fig. 6 *b*). Adopting the criterion that if the peak frequency of $\varepsilon''_q(f)$ is higher than 17 GHz, the solute is regarded as a water-structure breaker, the result is consistent with the order of strength of the structure-breaking effect obtained using other techniques (Robinson et al., 1996). These results strongly support our dielectric method which has enabled us to reveal this unique hydration property of actin.

In the first hydration shell of a protein, the mobility of water is generally lowered due to the interaction with residues on the protein surface (Bellissent-Funel, 1999; Halle and Denisov, 2001; Makarov et al., 2000; Mattos, 2002). In this respect, actin is not different from other proteins as outlined above. How then is the hyper-mobile state of water induced in actin? The surface of G-actin is rich in negative charges (Sheterline et al., 1998; Janmey et al., 2001), which could be responsible for inducing a hyper-mobility of water molecules that interact with such charges. This possibility, however, cannot be tested by the present dielectric spectroscopic techniques, because the dielectric spectrum of G-actin alone is practically immeasurable as noted above. An alternative view is that the induction of hyper-mobile water may be inherent to the F-actin structure. Using an x-ray structure-based three-dimensional model (Lorenz et al., 1993), the electrostatic potential for F-actin was predicted by recent simulations (Ouporov et al., 1999). This indicates that F-actin can be seen as a double helix of bulbs of negative potential extending into the solvent. Thus, F-actin may be likened to a charged cylinder (Oosawa, 1971). The strength

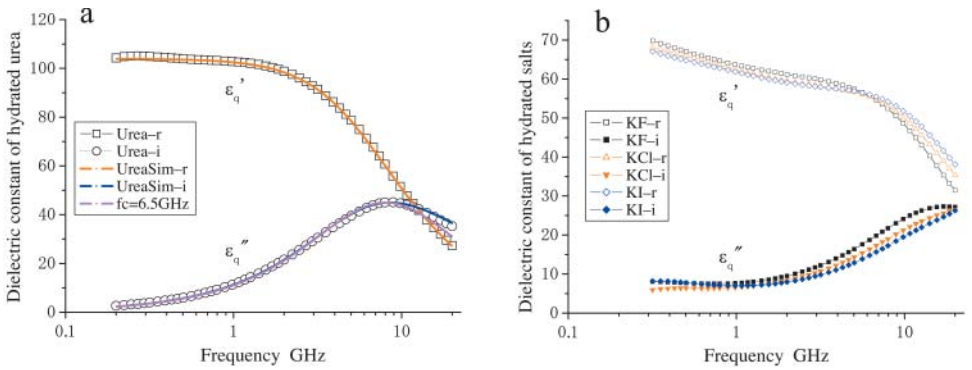

FIGURE 6 Dielectric spectra of hydrated solutes in urea and potassium halides solutions. (*a*) Experimental values for urea (ε'_q, *squares*; ε''_q, *circles*) measured in 2% (w/v) solution are superimposed with theoretical curves (*red* and *blue*) simulated with the two components combined together: one with $f_{c1} = 6.5$ GHz, $\delta_1 = 110$, and $N_1 = 2.4$; and the other with $f_{c2} = 30$GHz, $\delta_2 = 88$, and $N_2 = 2.4$ using Eqs. 1–5 and $N_{1,2} = \phi_{1,2}M_w/18c$. The magenta-colored curve is the spectrum (*imaginary part*) of the component with $f_{c1} =$ 6.5 GHz. (*b*) Spectra of potassium halide salts, KF (*black*), KCl (*red*), and KI (*blue*) measured in 0.2 M solutions. The curves were calculated using Eq. 5 with a constant $\phi_t = 0.117$, which was the largest among those of KF, KCl, and KI. The peak in ε''_q spectra are at 18 GHz for KF, whereas the simulation indicates peaks at $f_{c2} = 22$ GHz and 25 GHz for KCl and KI, respectively.

of its electric field would decay much less abruptly than that of a charged sphere. Hence, there may be a region in the vicinity of the cylinder surface where the strength of the electric field is comparable to that formed by large halide ions such as I^-. This may be the site where the hydrogen-bonded network of water is modulated. This would result in some of the bonds being short-lived and thereby enabling water molecules to become more mobile. To the best of our knowledge, the present work is the first to describe the presence of hyper-mobile water around a protein. Thus, it is important to examine whether or not this hypothesis is feasible using molecular dynamics and other related methods. If not, then the great challenge is to predict the structure of the actin molecule surface and/or the shape responsible for induction of such a large mass of hyper-mobile water.

Implication of hyper-mobile water in chemomechanical coupling

The diffusion coefficient of solute particles in water is inversely proportional to the viscosity of water, which is in a reciprocal relation with the rotational mobility of water molecules (Bloomfield, 2002; Fabelinskiĭ, 1997). Thus, our results suggest that a unique hydration shell containing water components with high and low viscosity is formed around F-actin (Fig. 7 *a*). Since the effect is undoubtedly structure-dependent, it would most likely undergo compositional fluctuations upon interaction with a specific binding protein. The binding proteins would induce characteristic conformational changes in the G-actin unit (Sheterline et al., 1998; Janmey et al., 2001) and some such changes would be cooperatively propagated through a filament (Oosawa et al., 1973; Orlova and Egelman, 1997). Thus, it is conceivable

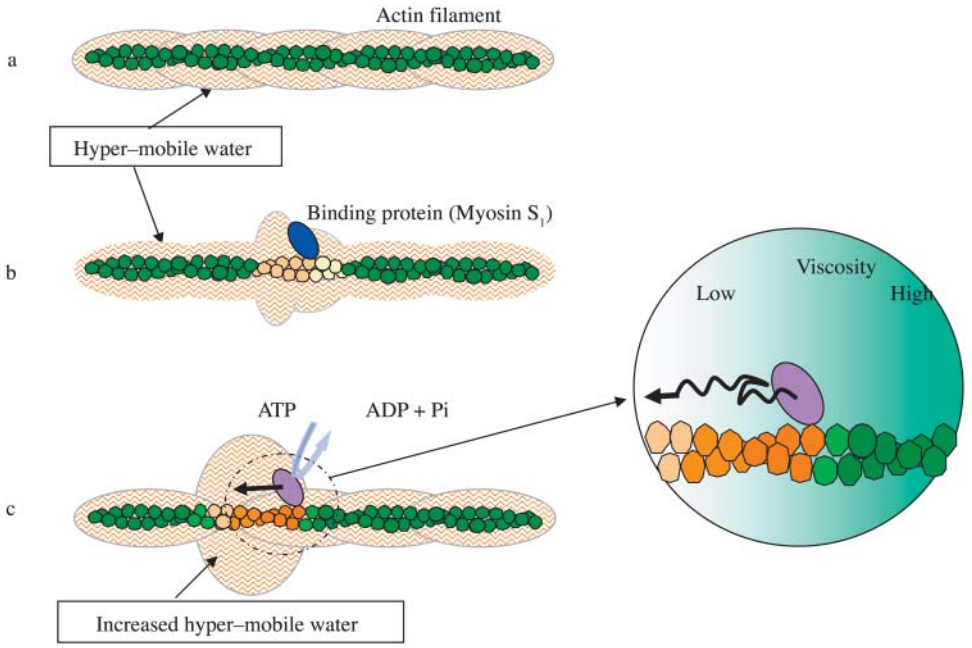

FIGURE 7 A diagrammatic representation of the idea underlying the hypothesis of unidirectional sliding of myosin along F-actin. (*a*) The surface of F-actin is covered by a layer of hyper-mobile water (for simplicity's sake, the ordinary restrained water is not shown). (*b*) Upon interaction with a specific binding protein, actin changes its conformation, which is in turn propagated directionally to adjacent monomers to generate solvent space of axially skewed viscosity. (*c*) During an ATP hydrolyzing cycle, myosin undergoes conformational changes in coupling with alternating strong and weak affinities for actin. The conformational changes are transmitted to actin and propagated as in *b*. Thus, the asymmetric space for diffusion is dynamically generated, where myosin moves toward the direction of lower viscosity.

that upon interaction with actin, certain binding proteins bring themselves in solvent space asymmetric in viscosity along the filament axis (Fig. 7 *b*). We propose that in muscle contraction, the energy resulting from ATP hydrolysis is ultimately converted into the viscosity anisotropy around each myosin interacting with the actin filament, which would facilitate the directional movement of myosin along the filament (Fig. 7 *c*). This offers an explanation for the key issue of the chemomechanical energy transduction: how the molecular motors work efficiently by breaking the symmetry of thermal motions of molecules even though the energy input only marginally exceeds the thermal energy.

We thank K. Asami, K. Sekine, F. Hirata, M. Irisa, T. Miyazaki, H. Takata, T. Yasunaga, S. Nishikawa, H. Higuchi, Y. Osada, and Y. Harada for discussions and support, and J. West for reading the manuscript.

This work was supported by Grant in Aid #11167203 from the Ministry of Education, Culture, Sports, Science and Technology of Japan.

REFERENCES

Asami, K., T. Hanai, and N. Koizumi. 1980. Dielectric analysis of *Escherichia coli* suspensions in the light of the theory of interfacial polarization. *Biophys. J.* 31:215–228.

Bellissent-Funel, M.-C. 1999. Hydration Process in Biology, NATO Science Series, Series A, Vol. 305. IOS Press, Amsterdam, The Netherlands.

Bloomfield, V. 2002. Survey of biomolecular hydrodynamics. *In* Separations, and Hydrodynamics. J. Correia, editor. Biophysical Society, Bethesda, MD. http://www.biophysics.org/btol/separat.html.

Bryant, R. G. 1996. The dynamics of water-protein interactions. *Annu. Rev. Biophys. Biomol. Struct.* 25:29–53.

Buchner, R., J. Barthel, and J. Stauber. 1999. The dielectric relaxation of water between 0°C, and 35°C. *Chem. Phys. Lett.* 306:57–63.

Collins, K. D. 1997. Charge density-dependent strength of hydration and biological structure. *Biophys. J.* 72:65–76.

Ellison, W. J., K. Lamkaouchi, and J. M. Moreau. 1996. Water: a dielectric reference. *J. Mol. Liq.* 68:171–279.

Fabelinskiĭ, I. L. 1997. Macroscopic and molecular shear viscosity. *Physics-Usppekhi.* 40:689–700.

Frank, H. S., and W. Y. Wen. 1957. Structural aspects of ion-solvent interaction in aqueous solutions: a suggested picture of water structure. *Disc. Faraday Soc.* 24:133–140.

Gregory, R. B. 1995. Protein-Solvent Interactions. Marcel Dekker, New York.

Halle, B., and V. P. Denisov. 2001. Magnetic relaxation dispersion studies of biomolecular solutions. *Meth. Enzymol.* 338:178–201.

Hayashi, Y., N. Miura, J. Isobe, N. Shinyashiki, and S. Yagihara. 2000. Molecular dynamics of hinge-bending motion of IgG vanishing with hydrolysis by papain. *Biophys. J.* 79:1023–1029.

Highsmith, S., K. Duignan, R. Cooke, and J. Cohen. 1996. Osmotic pressure probe of actin-myosin hydration changes during ATP hydrolysis. *Biophys. J.* 70:2830–2837.

Hribar, B., T. N. Southall, V. Vlachy, and K. A. Dill. 2002. How ions affect the structure of water. *J. Am. Chem. Soc.* 124:12302–12311.

Imai, T., H. Nomura, M. Kinoshita, and F. Hirata. 2002. Partial molar volume and compressibility of alkali-halide ions in aqueous solution: hydration shell analysis with an integral equation theory of molecular liquids. *J. Phys. Chem. B.* 106:7308–7314.

Janmey, P. A., J. X. Tang, and C. F. Schmidt. 2001. Actin filaments. *In* Supramolecular Assemblies, Chapter 5. V. Bloomfield, editor. Biophysical Society, Bethesda, MD. http://www.biophysics.org/btol/supramol.html.

Kaatze, U. 1990. On the existence of bound water in biological systems as probed by dielectric spectroscopy. *Phys. Med. Biol.* 35:1663–1681.

Kouyama, T., and K. Mihashi. 1981. Fluorimetry study of *n*-(1-pyrenyl) iodoacetamide-labelled F-actin. Local structural change of actin protomer both on polymerization and on binding of heavy meromyosin. *Eur. J. Biochem.* 114:33–38.

Lorenz, M., D. Popp, and K. C. Holmes. 1993. Refinement of the F-actin model against x-ray fiber diffraction data by the use of a directed mutation algorithm. *J. Mol. Biol.* 234:826–836.

Makarov, V. A., B. K. Andrews, P. E. Smith, and B. M. Pettitt. 2000. Residence times of water molecules in the hydration sites of myoglobin. *Biophys. J.* 79:2966–2974.

Mattos, C. 2002. Protein-water interactions in a dynamic world. *Trends Biochem. Sci.* 27:203–208.

Oosawa, F. 1971. Polyelectrolytes. Marcel Dekker, New York.

Oosawa, F., S. Fujime, S. Ishiwata, and K. Mihashi. 1973. Dynamic property of F-actin and thin filament. *Cold Spring Harb. Symp. Quant. Biol.* 37:277–285.

Orlova, A., and E. H. Egelman. 1997. Cooperative rigor binding of myosin to actin is a function of F-actin structure. *J. Mol. Biol.* 265:469–474.

Ouporov, I. V., H. R. Knull, and K. A. Thomasson. 1999. Brownian dynamics simulations of interactions between aldolase and G- or F-Actin. *Biophys. J.* 76:17–27.

Robinson, G. W., S. B. Zhu, S. Singh, and M. W. Evans. 1996. Water in Biology, World Scientific Series in Contemporary Chemical Physics, Vol. 9. World Scientific, Singapore.

Samoilov, O. Y. 1957. A new approach to the study of hydration of ions in aqueous solutions. *Disc. Faraday Soc.* 24:141–146.

Sheterline, P., J. Clayton, and J. C. Sparrow. 1998. Actin, 4th Ed. Oxford University, Oxford, UK.

Spudich, J. A., and S. Watt. 1971. The regulation of rabbit skeletal muscle contraction. 1. Biochemical studies of the interaction of the tropomyosin-troponin complex with actin and the proteolytic fragments of myosin. *J. Biol. Chem.* 246:4866–4871.

Suzuki, M., J. Shigematsu, and T. Kodama. 1996. Hydration study of proteins in solution by microwave dielectric analysis. *J. Phys. Chem.* 100:7279–7282.

Suzuki, M., J. Shigematsu, Y. Fukunishi, and T. Kodama. 1997a. Hydrophobic hydration analysis on amino acid solution by the microwave dielectric method. *J. Phys. Chem. B.* 101:3839–3845.

Suzuki, M., J. Shigematsu, Y. Fukunishi, Y. Harada, T. Yanagida, and T. Kodama. 1997b. Coupling of protein surface hydrophobicity change to ATP hydrolysis by myosin motor domain. *Biophys. J.* 72: 18–23.

Tovchigrechko, A. D., M. N. Rodnikova, and J. Barthel. 1999. Comparative study of urea and tetramethylurea in water by molecular dynamics simulation. *J. Mol. Liq.* 79:187–201.

Wüthrich, K. 2001. The way to NMR structures of proteins. *Nature (Struct. Biol.)* 8:923–925.

Yokoyama, K., T. Kamei, H. Minami, and M. Suzuki. 2001. Hydration study of globular proteins by microwave dielectric spectroscopy. *J. Phys. Chem. B.* 105:12622–12627.

Zhou, H. X. 2001. A unified picture of protein hydration: prediction of hydrodynamic properties from known structures. *Biophys. Chem.* 93: 171–179.